SiliconPV 2015
PC1Dmod 6.1 - state-of-the-art models in a well-known interface for improved simulation of Si solar cells

Halvard Haug[1] Johannes Greulich[2], Achim Kimmerle[2] and Erik Stensrud Marstein[1]

[1] Institute for Energy Technology, Instituttveien 18, 2007 Kjeller, Norway.
Phone: +47 63806233, E-mail: halvard.haug@ife.no

[2] Fraunhofer Institute for Solar Energy Systems, Heidenhofstraße 2, 79110 Freiburg, Germany

Abstract

In this paper, we present a new, updated version of the commonly used semiconductor device simulator PC1D named PC1Dmod 6.1. The new program is based on the previously published command line version cmd-PC1D 6.0, which has implemented several new options related to the device physics, but now uses an updated version of the original PC1D graphical user interface. The program thus provides the possibility for using Fermi-Dirac statistics and a selection of state-of-the-art models for crystalline silicon, including injection-dependent band gap narrowing, carrier mobility and Auger recombination, in a familiar setting.

Version 6.1 also has implemented the recently published band gap narrowing model by Yan and Cuevas, which is based on empirical studies of a large selection of both n^+ and p^+ emitters, in addition to Schenk's model. It has also implemented the mobility model for compensated material by Schindler $et\ al$. Finally, the maximum number of nodes, time steps and wavelengths has been increased in order to reduce unnecessary constraints on simulations and external files.

The results from the PC1Dmod 6.1 simulations have been compared with those of other simulation tools and with previously published data to verify the correct implementation of the new models. Emitter saturation currents calculated using PC1Dmod 6.1 showed an excellent agreement with those obtained using the emitter recombination calculator EDNA 2, and the new program was able to successfully reproduce previously published experimental data and previous implementations of the models. Both PC1Dmod 6.1 and the command line version cmd-PC1D 6.1 are open source software, and are freely available for download.

Keywords: Silicon, Device simulation, Solar cell, Fermi-Dirac statistics

1. Introduction

PC1D is an efficient, one-dimensional semiconductor device simulator which has strongly influenced the solar cell research community [1], [2]. The program uses a finite-element numerical method for solving the coupled nonlinear equations for carrier generation, recombination and transport in the device. It can be applied both for simulation of device performance and as a tool for new users to understand the fundamentals of solar cell physics. The main advantages of PC1D include a high calculation speed, an intuitive user interface and an extensive list of material and physical parameters. By varying the applied bias or the wavelength of the excitation light source, PC1D can calculate both current-voltage characteristics and the spectral quantum efficiency of the solar cell, but it also has a large number of other options for output data, both in the spatial domain and in the time domain.

The carrier statistics in PC1D is based on the Boltzmann approximation, and several PV-specific models have been developed for use in this framework. However, since electrons are Fermions, they obey Fermi-Dirac (F-D) statistics. F-D statistics should therefore generally be used (together with a correct description of the band structure and the density of states) to obtain correct simulation results. Recently, we developed a modified version of the program called cmd-PC1D 6.0, which extends the original program by implementing F-D statistics [3]. Furthermore, models for various properties of crystalline silicon (c-Si) have been refined and improved since the latest official release of PC1D in 1997. We therefore also implemented several

advanced Si-specific models into cmd-PC1D 6.0 in order to improve the accuracy of simulations of c-Si devices. An update that was of particular importance was the model for band gap narrowing (BGN), as the effect of carrier degeneracy at high doping levels (which is not accounted for with Boltzmann statistics) was previously compensated for by the use of an *apparent* BGN model. A list of the currently implemented state-of-the-art models for c-Si is provided later in this paper (Section 3).

For practical reasons, the changes to the device physics have previously been implemented in a simplified, command line version of PC1D which gives additional possibilities for scripting simulations. However, this flexibility comes with a requirement of a certain degree of programming skills for the user, or alternatively, the need to use a compiled Matlab program as an alternative graphical user interface, which was also provided [4]. As a response to several requests from the solar cell research community, we now present a new version of the program called PC1Dmod 6.1, which implements the new physical models into an updated version of the original GUI. Additionally, new Si models for BGN in highly doped regions, mobility in compensated material and position-dependent Shockley-Read-Hall recombination have been added, in addition to some numerical improvements.

The present paper is organized as follows. In section 2 we give a short overview of the F-D implementation and the new physical models which were introduced in cmd-PC1D.6.0 [3]. In section 3 the models newly introduced in this work (version 6.1) are described. In section 4 we verify that the latest models have been correctly implemented by comparing the results to other well-accepted simulation tools and previously published data. In section 5 we provide some details on the changes made to the user interface and on the configuration of physical models, as well as changes to the c-Si material files and to the numerical constraints of the program. In section 6 possible further work is discussed. The key results of the present work are summarized in in section 7.

2. Fermi-Dirac statistics and physical models introduced in version 6.0

The performance of solar cells is strongly affected by carrier recombination, which again depends on the excess concentration of minority carriers. Because of this, both the pn product and the recombination processes in the device must be known precisely in order to obtain accurate simulation results. The pn product at equilibrium scales as the square of the intrinsic carrier density n_i, and at large doping densities it is also significantly influenced by degeneracy and BGN. In order to correctly account for the statistical effects of electrons being Fermions, which become particularly apparent at carrier concentrations larger than 1e18 cm-3, Fermi-Dirac statistics should be used [5]. F-D statistics is now used as default in PC1Dmod, using the same implementation that was introduced for cmd-PC1D 6.0. Interested readers are referred to our previous publication [3] for a more detailed description.

The models used in PC1D 5.9 have been developed for use together with Boltzmann statistics, and should therefore be re-evaluated when changing to F-D statistics. This is particularly true for BGN, as the current models used in PC1D represent the *apparent* BGN, which accounts for various effects, including degeneracy at high doping levels. Because of this we cannot apply F-D statistics together with the existing BGN models, as this would overestimate the high doping effects. Instead, the BGN is calculated using the comprehensive theoretical model for both *p*- and *n*-type Si by Schenk [6], which is derived for the case of F-D statistics from a non-self-consistent, full random phase approximation formalism, taking both carrier–carrier and carrier–dopant interactions into account. Schenk's model also accounts for BGN in the base substrate due to injected carriers, which can have a significant effect in devices and lifetime samples at high injection conditions [7].

The Schenk BGN model takes part in a collection of state-of-the-art models for (highly doped) c-Si which were chosen for use in cmd-PC1D 6.0 [3] as suggested by Altermatt et al. [5][8]. This set of models also includes Sproul and Green's model for the temperature-dependent intrinsic carrier density $n_{i,0}(T)$ [9], which has been linearly scaled by a constant factor 0.9677 to match the latest value of 9.65×10^9 cm-3 at 300 K as reported by Altermatt *et al.* [10], as well as the extensive and commonly used mobility model by Klaassen

[11], [12]. Furthermore, we have also implemented the latest parameterisation of intrinsic recombination by Richter *et al.* [13], which was derived using F-D statistics and Schenk's parameterization for BGN, and is based on a large set of empirical data, taking the latest advances in material quality and surface passivation into account. As an alternative we have also implemented the also commonly used model by Kerr and Cuevas [14] for intrinsic recombination. The current selection of new models implemented in PC1Dmod 6.1 is given in Table I. More details on the choice of models and their implementation can be found in Ref. [3].

3. Physical models added in version 6.1

The framework for implementing new models and a simple configuration of which models and parameters to use is now in place in the PC1Dmod program, and additional options for physical models can therefore be included in a simple manner, thus meeting the needs of different users and enabling the program to follow the latest scientific progress.

A clear example of an ongoing scientific debate is the discussion of how to simulate carrier recombination in the highly doped surface regions in Si solar cells, and the role of the band gap narrowing in this regard. Recently, Yan and Cuevas have published an empirical BGN model for 300 K based on fitting of measured emitter saturation current densities for a large selection of n^+ and p^+ dopant profiles determined by electrochemical capacitance-voltage measurements [15], [16]. There is an ongoing discussion in the scientific community regarding the differences in the theoretical (Schenk BGN and F-D statistics) and empirical (effective BGN and Boltzmann/F-D statistics) approach to simulate highly doped regions in silicon. In order to provide users with additional options and to improve the predictive powers of the program, the empirical model of Yan and Cuevas has now been implemented in PC1Dmod 6.1 as an alternative to Schenk's BGN model (See Table 1). The program thus provides a base for expert users to test the two different views in comparing simulation and measured data.

Another important update in PC1Dmod 6.1 is the inclusion of the charge carrier mobility model by Schindler *et al.* [17] for compensated silicon. The carrier mobility in compensated Si is reduced as compared to uncompensated material. In order to better be able to simulate devices produced from compensated Si wafers we have implemented the extensive model of Schindler *et al.* [17], which extends Klaassen's mobility model [11], [12] with additional scattering terms to fit a large set of experimental mobility data measured on compensated material. For uncompensated material, Schindler's merges with Klaassen's at high and low temperature, but adds an additional exponential term to the hole mobility from scattering at phonons in order to correct for an observed deviation between the model an experimental data in the temperature range between 80 K and 300 K.

Model	Symbol	Ref.	
Intrinsic carrier density	$n_{i,0}(T)$	Altermatt et al. 2003	[10]
Intrinsic energy band gap	$E_{g,0}(T)$	Green 1990	[18]
Effective density of states, conduction band	N_c	Green 1990	[18]
Effective density of states, valence band	N_v	(adjusted to match $n_{i,0}$)	
Bandgap narrowing	$\Delta E_c, \Delta E_v$	Schenk 1998	[6]
		Yan and Cuevas 2013 *	[15]
		Yan and Cuevas 2014 *	[16]
Carrier mobility	μ_n, μ_p	Klaassen 1992	[11],[12]
		Schindler 2014 *	[17]
Intrinsic recombination	U_{intr}	Richter et al. 2012	[13]
		Kerr and Cuevas 2002	[14]
Numerical approximations for:			
Fermi integral	$u = F_{1/2}(\eta)$	Van Halen and Pulfrey 1985	[19]
Inverse Fermi integral	$\eta = f_{1/2}(u)$	Antia 1993	[20]

Table. 1.

Overview of the new Si models in PC1Dmod and cmd-PC1D. (*) = New models in version 6.1.

4. Verification of new models

In order to verify that the newly included models have been implemented correctly, a series of simulations have been performed using PC1Dmod 6.1 and the results have been compared with other simulation tools and previously published data.

4.1. Band gap narrowing

Fig. 1 shows the BGN in boron doped c-Si as a function of the concentration of acceptor dopants. The empirical BGN model of Yan and Cuevas [16] predicts a larger BGN than the theoretical model by Schenk [6]. Note also that the *apparent* BGN model which is derived using Boltzmann statistics is lower than the one based on F-D statistics, as this also takes carrier degeneracy into account. The previous BGN model used as default in PC1D 5.9 is also shown for comparison. The parameterization used the work and Yan and Cuevas and in PC1D 5.9 can be written as
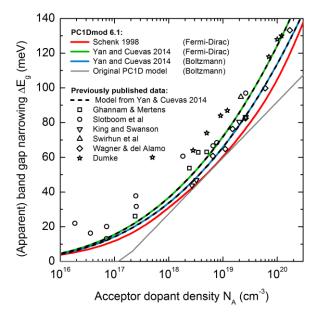
$$\Delta E_g = A \times \left[\ln \left(\frac{N_{dop}}{N_{ref}} \right) \right]^b, \tag{2}$$

where N_{dop} is the doping concentration N_D or N_A for n-type or p-type material, respectively. The values used for the parameters A, b and N_{ref} are given in Table 2 below. Note that for Boltzmann statistics the exponent was set to $b = 1$ in Ref. [15] for n-type material and $b = 3$ in Ref. [16] for p-type material. These values are therefore also used in the current version of PC1Dmod.

BGN model	BGN type	Carrier statistics	A (meV)	b	N_{ref} (cm^{-3})
Yan & Cuevas	N_D	F-D	0.0420	3	1×10^{14}
		Boltzmann	12.96	1	1×10^{17}
	N_A	F-D	0.0472	3	1×10^{14}
		Boltzmann	0.0432	3	1×10^{14}
PC1D 5.9 *	N_D/N_A	Boltzmann	14.00		1.4×10^{14}
Schenk	$N_D/N_A/\Delta n$	F-D	-	-	-

Table. 2.

List of (effective) BGN models and parameters used in PC1Dmod 6.1. *The effective BGN parameters used for PC1D 5.9 were intended to use with $n_i = 1 \times 10^{10}$ cm^{-3}, whereas the other parameters should be used with $n_i = 9.65 \times 10^9$ cm^{-3} at 300 K.
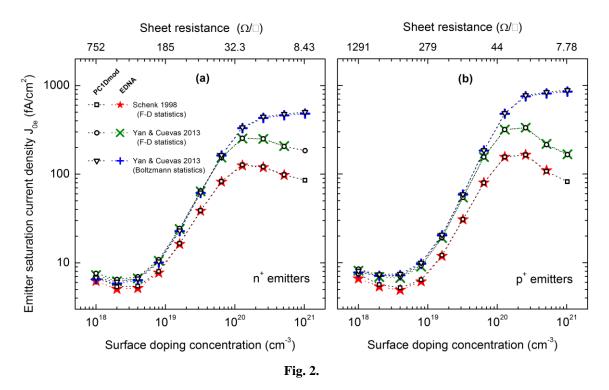

Fig. 1.

A comparison of BGN models as a function of acceptor concentration in boron doped p-type Si. Solid lines are calculated with PC1Dmod 6.1, black dashed lines (model) and open symbols (experimental literature data) are reproduced from Ref. [16]. Note that electrical BGN measurements [21]–[24] were recalculated using Klaassen's mobility model and $n_i = 9.65 \times 10^9$ cm^3 in Ref. [16], whereas the photoluminescence measurements [25], [26] are shown with their original values. Note that the effective BGN used for PC1D 5.9 were intended to use with $n_i = 1 \times 10^{10}$ cm^{-3}.

To verify that the BGN models have been implemented correctly we performed simulations of the emitter saturation current J_{0e} for a series of n-type and p-type Gaussian diffusions with different surface doping concentration and compared the results to those obtained with the numerical simulation tool EDNA 2 [27]. A fixed standard deviation of 0.2 μm was used for all the dopant profiles and the surface recombination velocity (SRV) parameter S_{p0} was set as a function of the surface doping concentration according to the parameterization of Altermatt *et al.* [5] of the data of Cuevas *et al.* for Si passivated with SiO_2 [28]. (See Ref. [3] for further details on the J_{0e} simulations and other device parameters). Fig. 2 shows the J_{0e} values simulated using the Schenk BGN and both Boltzmann and F-D versions of the Yan and Cuevas BGN model. An excellent agreement is observed between PC1Dmod 6.1 and EDNA in all the calculated values. In addition to the BGN, these results also depend on the carrier mobility, intrinsic recombination and band structure parameters, indicating that all of these models have been implemented correctly. PC1Dmod 6.1 is thus able to produce the same results as EDNA, but with the added benefit of being able to use the same recombination behavior directly into simulations of full solar cell devices and lifetime samples. In addition, PC1D also has the capability to account for additional band bending arising from surface charges in the passivation, which is currently not possible in EDNA.
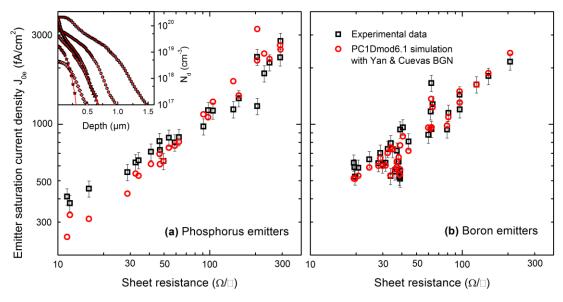
Note that the Yan and Cuevas BGN model produces significantly larger J_{0e} values as compared to the Schenk BGN when using the same values for the SRV parameter S_{0p}. In practice however, the difference in J_{0e} is usually accounted for by adapting S_{0p} to match experimental data, meaning that similar recombination properties may be obtained from both models, but with a different ratio between the contributions from surface recombination and from Auger recombination in the highly doped surface region.

Fig. 2.

Calculated J_{0e} values as a function of surface doping density for n-type (a) and p-type (b) emitters (Gaussian profiles, fixed standard deviation of 0.2 μm). Simulation results from PC1Dmod 6.1 (open symbols) show an excellent agreement with EDNA 2 (closed symbols). Note that the same parameterization for S_{0p} as a function of N_{surf} has been used in all cases.

In the extraction of the Yan and Cuevas BGN model [15], [16] the issue of unknown SRV was circumvented by performing the experimental J_{0e} measurements on samples covered with a very thin layer of aluminum, which is meant to ensure that the SRV is fixed at a large value equal to the thermal velocity of the carriers (taken as $S_{0p} = 3 \times 10^6$ cm/s). The BGN parameters were then extracted by matching the experimental J_{0e} values to an analytical J_{0e} calculation using the same models for the intrinsic carrier density, carrier mobility and Auger recombination as shown in Table I. (For the extraction of empirical BGN of n+ emitters in Ref. [15], an older Auger parameterization [14] were used. However, because of the large SRV in the experiment, the choice of Auger parameterization is only of minor importance for the extracted BGN parameters).

PC1Dmod 6.1 was also used to perform J_{0e} simulations based on the original data for the phosphorous and boron doping profiles used in of Refs. [15] and [16], respectively. This attempt to reproduce the experimental J_{0e} values that were used as a starting point for the BGN parameterization in the first place was done in order to further verify the correct implementation of the models and to demonstrate the predictive capabilities of the program. Fig. 3 shows a comparison between the simulation results and the measured data, showing a good agreement for most of the doping profiles. Some deviation is observed for the heaviest (lowest sheet resistance) n+ emitters, which can mostly be attributed to the fact that one global set of BGN parameters were used for the simulations, which is based on the average value from all the measurements shown in the figure. For the p+ emitters we observe a very good correspondence for the entire range of doping profiles. As an example of the advantages of command line simulations, we want to note that all the simulations shown in Fig. 3 were performed using cmd-PC1D 6.1 running within a script, resulting in a total computation time of less than 30 seconds for the entire data set.

Fig. 3.

Comparison of measured and simulated J_{0e} values for a range of different diffused phosphorus (a) and boron (b) dopant profiles covered with a thin layer of aluminum. Experimental doping profiles and J_{0e} values are the original data from Refs. [15] and [16], respectively, with the error bars representing a $\pm 10\%$ error in the measurements. The simulated data points are calculated using PC1Dmod 6.1 as described in the text, using the Yan and Cuevas BGN model for each doping type, a fixed SRV of 3×10^6 cm/s and other parameters as described in Refs. [15] and [16]. Inset: A selection of n$^+$ doping profiles, from the minimum to the maximum sheet resistance shown in (a).

4.2. Position-dependent SRH recombination

One fundamental assumption that was used when extracting the Yan and Cuevas BGN model was that the recombination in the bulk of the emitters is dominated by Auger recombination, and Shockley-Read Hall (SRH) recombination was therefore neglected in the calculations. Min *et al.* [29] recently suggested that SRH recombination close to the surface actually is an important contributing factor for the total J_{0e}, and can therefore be used to explain the observed differences in simulated and experimental J_{0e} data for the cases when only adapting S_{0p} is not sufficient. Resolving the discussion of which BGN model that should be used for device simulation and the potential role of SRH recombination in solar cell emitters is beyond the scope of this paper. We however want to provide a new tool for further investigation in this topic, and have therefore also implemented an option for adding position-dependent SRH recombination, which is defined by importing a text file specifying the SRH time constants τ_{0n} and τ_{0p} at different positions. In order to verify the implementation and to demonstrate a potential use of this feature we have used PC1Dmod 6.1 simulations to reproduce the original data published in the work of Min *et al.* [29], which simulated the J_{0e} values of a series of emitters fabricated on planar substrates. The additional SRH recombination in the emitter was assumed to be proportional to the concentration of inactive phosphorus at each point, taken as the difference between secondary ion mass spectrometry (SIMS) and electrochemical capacitance-voltage (ECV) measurements, which measures the concentration of total and active dopants, respectively. As in Ref. [29] the SRV (via the S_{0p} parameter) were adjusted to best match the experimental J_{0e} values for each of four different emitters produced with increasing POCl$_3$ flow during phosphorus diffusion. As seen in Fig. 4, it was not possible to reproduce the measured J_{0e} data using the Schenk BGN model, even by setting S_{0p} to the maximum value of 1.56×10^7 cm/s suggested in Ref. [5]. Using the Yan and Cuevas BGN the simulated J_{0e} values for a given S_{0p} are higher, and the simulations could be matched to the experimental data by adapting S_{0p}, except for the heaviest emitter, where this model also fails to account for the measured value. However, by including SRH recombination and using a single value for the effective capture cross section of the assumed defect of $\sigma_p = 8 \times 10^{-18}$ cm^2 it was possible to obtain a good agreement with the experiment, also when using Schenk's BGN model. (Note that this value for σ_p is slightly different than the value 7.5×10^{-18} cm^2 used in Ref. [29], probably caused by the use of slightly different band structure parameters at 25 ℃).
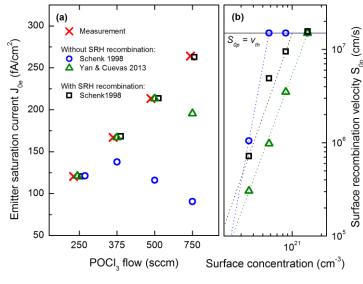

Fig. 4.

(a) J_{0e} measurements (red crosses) as a function of POCl$_3$ flow during the diffusion process, from Ref [30] and later reevaluated in Ref. [29]. The simulated J_{0e} is calculated at 25 ℃ using both the Schenk and Yan & Cuevas BGN models, and show a best fit to the measurements by adapting S_{0p} in each case, as shown in (b). Dashed lines show the best fit of the S_{0p} values to the parameterization described in Ref. [5].

4.3. Mobility in compensated c-Si

Fig. 5 shows the electron and hole mobility in c-Si as a function of doping density for uncompensated and heavily compensated c-Si. The mobility values calculated in PC1Dmod 6.1show a perfect agreement with the VBA implementation of the model by the author of Refs. [31] and [17], again indicating that PC1Dmod 6.1 evaluates these values correctly. Device simulation on compensated c-Si material is an interesting field and will hopefully be one topic for further development of PC1Dmod in the near future.
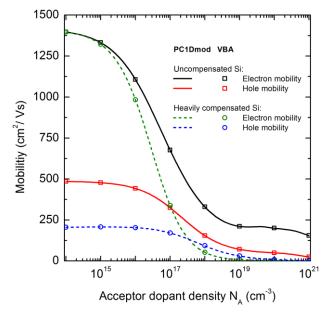

Fig. 5.

Charge carrier mobility as a function of acceptor doping density, for uncompensated ($N_A = 10^{16}$ cm^{-3}) and heavily compensated ($N_A = 10^{17}$ cm^{-3}, $N_D = 9 \times 10^{16}$ cm^{-3}) c-Si, calculated using the mobility model by Schindler [17] in PC1Dmod 6.1 (lines) and the original VBA implementation of the model (symbols).

5. Other changes in PC1Dmod 6.1

5.1. User interface

Only a few small changes have been done to the original user interface in PC1Dmod 6.1, mostly for practical and cosmetic reasons. To clearly distinguish PC1Dmod 6.1 from the official PC1D 5.9 program a blue background color has been added, and the graph window colors have been changed to a more modern theme with white background. The parameter section has also been updated to clearly indicate when the original PC1D material parameters and models are not in use.

The most important change in PC1Dmod 6.1 is the introduction of a separate configuration file, which lets the user specify which models and parameters to use. All available keyword options can be included in the last part of the file for easy reference, or they can be looked up in the updated help file which is distributed alongside the program. Different configuration files can be loaded, edited and saved using shortcuts within the PC1Dmod program. When choosing Boltzmann statistics and the original PC1D models the results from the original PC1D 5.9 program are reproduced.

5.2. Other material properties for c-Si

In the original PC1D program, all material parameters were stored in a .mat file. As default, many of these properties have now been replaced by globally defined, c-Si specific models as described in sections 3 and 4. However, not all changes in c-Si material properties have been directly included into the PC1Dmod 6.1 program, and some properties, like the refractive index and optical absorption coefficient, are still stored in external data files as before. PC1Dmod 6.1 is therefore distributed together with an updated set of external files for c-Si regarding these important properties, as described in Ref. [32]. Furthermore, updated parameters for free-carrier absorption, as published by Rüdiger et al. [33], have been used as default in the included .prm files.

5.3. Numerical improvements

Major advances in computation power have happened since the release of PC1D 5.9 in 1997, and many of the computational limitations of the original program are therefore no longer relevant. The addition of F-D statistics and injection-dependent models (which must be evaluated at each iteration) has resulted in some loss of computation speed in PC1Dmod 6.1, but simulations are still very fast on modern computers. Therefore it was natural to also increase some of the numerical constraints imposed in the original program, regarding external file lengths (increased to 1000 lines), number of transient steps (increased to 1000 steps) and node density (maximum number of elements increased from 500 to 5000). PC1D5.9 has implemented an efficient renoding algorithm, but the program sometimes suffered from the fact that the node density in the initial state was too limited to accurately reflect external doping profiles, which are sampled before any renoding occurs. In PC1Dmod 6.1 the initial node density is also increased by a factor of 10, and the program thus reflects abrupt changes in external files more accurately. An example of this is presented in Fig. 6, which shows the sampling of an external emitter profile (applied for the emitter with $POCl_3 = 500$ sccm in Fig. 4), using both PC1D 5.9 and PC1Dmod 6.1

Finally, the physical constants used in PC1Dmod have been changed to their latest and most accepted values, available at the NIST online reference [34].
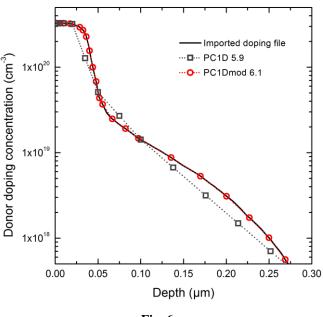

Fig. 6.

Illustration of the improved initial node density in PC1Dmod 6.1 (red circles), resulting in correct sampling of an external emitter profile imported from a text file (solid line). The original PC1D program (grey squares) could in some cases produce incorrect results because of too coarse interpolation.

7. Conclusion

In this paper we successfully verified the implementations of F-D statistics and new c-Si models for intrinsic carrier density, mobility, Auger recombination, band gap narrowing and position-dependent SRH recombination into PC1Dmod 6.1, a modified version of the original PC1D user interface. The empirical band gap narrowing model of Yan and Cuevas [15], [16] has been implemented as an alternative to the theoretical model by Schenk [6] and the mobility model by Schindler *et al.*[17] has been implemented in order to enable evaluation of the carrier mobility in compensated material. We demonstrated the agreement of emitter saturation currents for several Gaussian dopant concentration profiles calculated using PC1Dmod 6.1 with the established simulation tool EDNA 2 and show that the new program is able to reproduce previously published data and model implementations relevant for the included models. In summary, the correct implementation of both F-D statistics and several new physical models in PC1Dmod 6.1 has been successfully demonstrated.

The new program comes with a simple configuration of which models to use and will therefore hopefully lower the barrier for many researchers and engineers to utilize state-of-the-art physical models for device simulations. PC1Dmod 6.1 provides expert users with an open-source base to compare different models and verify them against experimental data, and at the same time giving less experienced users a possibility to access a well-checked, updated and meaningful preset of models in a familiar setting. PC1Dmod 6.1 is therefore likely to broaden the use of up-to-date models and to stimulate the discussion on their choice in the PV community. We hope that it may be a platform for future development, collaboration and discussion regarding simulation of Si solar cell devices.

PC1Dmod 6.1 is freely available for download and is currently hosted by PV Lighthouse (http://www.pvlighthouse.com.au/). The simplified command line version cmd-PC1D is also updated to version 6.1, and this program and the accompanying user interface PC1D for Matlab are also available through the same website. Finally, the source code of PC1Dmod 6.1 is available at www.sourceforge.net.

Acknowledgements

References

[1]   D. A. Clugston and P. A. Basore, "PC1D version 5: 32-bit solar cell modeling on personal computers," *Photovoltaic Specialists Conference, 1997., Conference Record of the Twenty-Sixth IEEE*. pp. 207–210, 1997.

[2]   P. A. Basore, "Numerical modeling of textured silicon solar cells using PC-1D," *Electron Devices, IEEE Transactions on*, vol. 37, no. 2. pp. 337–343, 1990.

[3]   H. Haug, A. Kimmerle, J. Greulich, A. Wolf, and E. Stensrud Marstein, "Implementation of Fermi–Dirac statistics and advanced models in PC1D for precise simulations of silicon solar cells," *Sol. Energy Mater. Sol. Cells*, vol. 131, no. 0, pp. 30–36, Dec. 2014.

[4]   H. Haug, B. R. Olaisen, Ø. Nordseth, and E. S. Marstein, "A Graphical User Interface for Multivariable Analysis of Silicon Solar Cells Using Scripted PC1D Simulations," *Energy Procedia*, vol. 38, pp. 72–79, 2013.

[5]   P. P. Altermatt, J. O. Schumacher, A. Cuevas, M. J. Kerr, S. W. Glunz, R. R. King, G. Heiser, and A. Schenk, "Numerical modeling of highly doped Si:P emitters based on Fermi–Dirac statistics and self-consistent material parameters," *J. Appl. Phys.*, vol. 92, no. 6, p. 3187, Aug. 2002.

[6]   A. Schenk, "Finite-temperature full random-phase approximation model of band gap narrowing for

silicon device simulation," *J. Appl. Phys.*, vol. 84, no. 7, p. 3684, 1998.

[7]   A. Kimmerle, P. Rothhardt, A. Wolf, and R. A. Sinton, "Increased Reliability for J0-analysis by QSSPC," *Energy Procedia*, vol. 55, pp. 101–106, 2014.

[8]   P. Altermatt, "Models for numerical device simulations of crystalline silicon solar cells—a review," *J. Comput. Electron.*, vol. 10, no. 3, pp. 314–330, 2011.

[9]   A. B. Sproul and M. A. Green, "Intrinsic carrier concentration and minority-carrier mobility of silicon from 77 to 300 K," *J. Appl. Phys.*, vol. 73, no. 3, p. 1214, Feb. 1993.

[10]   P. P. Altermatt, A. Schenk, F. Geelhaar, and G. Heiser, "Reassessment of the intrinsic carrier density in crystalline silicon in view of band-gap narrowing," *J. Appl. Phys.*, vol. 93, no. 3, p. 1598, Feb. 2003.

[11]   D. B. M. Klaassen, "A unified mobility model for device simulation—I. Model equations and concentration dependence," *Solid. State. Electron.*, vol. 35, no. 7, pp. 953–959, 1992.

[12]   D. B. M. Klaassen, "A unified mobility model for device simulation—II. Temperature dependence of carrier mobility and lifetime," *Solid. State. Electron.*, vol. 35, no. 7, pp. 961–967, 1992.

[13]   A. Richter, S. W. Glunz, F. Werner, J. Schmidt, and A. Cuevas, "Improved quantitative description of Auger recombination in crystalline silicon," *Phys. Rev. B*, vol. 86, no. 16, p. 165202, Oct. 2012.

[14]   M. J. Kerr and A. Cuevas, "General parameterization of Auger recombination in crystalline silicon," *J. Appl. Phys.*, vol. 91, no. 4, pp. 2473–2480, Feb. 2002.

[15]   D. Yan and A. Cuevas, "Empirical determination of the energy band gap narrowing in highly doped n+ silicon," *J. Appl. Phys.*, vol. 114, no. 4, p. 044508, 2013.

[16]   D. Yan and A. Cuevas, "Empirical determination of the energy band gap narrowing in p+ silicon heavily doped with boron," *J. Appl. Phys.*, vol. 116, no. 19, p. 194505, Nov. 2014.

[17]   F. Schindler, M. Forster, J. Broisch, J. Schön, J. Giesecke, S. Rein, W. Warta, and M. C. Schubert, "Towards a unified low-field model for carrier mobilities in crystalline silicon," *Sol. Energy Mater. Sol. Cells*, vol. 131, pp. 92–99, Dec. 2014.

[18]   M. A. Green, "Intrinsic concentration, effective densities of states, and effective mass in silicon," *J. Appl. Phys.*, vol. 67, no. 6, p. 2944, Mar. 1990.

[19]   P. Van Halen and D. L. Pulfrey, "Accurate, short series approximations to Fermi–Dirac integrals of order −1/2, 1/2, 1, 3/2, 2, 5/2, 3, and 7/2," *J. Appl. Phys.*, vol. 57, no. 12, p. 5271, 1985.

[20]   H. M. Antia, "Rational Function Approximations for Fermi-Dirac Integrals," *Astrophys. J. Suppl.*, vol. 84, pp. 101–108, 1993.

[21]   J. W. Slotboom and H. C. de Graaff, "Measurements of bandgap narrowing in Si bipolar transistors," *Solid. State. Electron.*, vol. 19, no. 10, pp. 857–862, Oct. 1976.

[22]   S. E. Swirhun, Y. H. Kwark, and R. M. Swanson, "Measurement of electron lifetime, electron mobility and band-gap narrowing in heavily doped p-type silicon," *Electron Devices Meeting, 1986 International*, vol. 32. pp. 24–27, 1986.

[23]   R. R. King and R. M. Swanson, "Studies of diffused boron emitters: saturation current, bandgap narrowing, and surface recombination velocity," *Electron Devices, IEEE Transactions on*, vol. 38, no. 6. pp. 1399–1409, 1991.

[24]   M. Y. Ghannam and R. P. Mertens, "Accurate determination of bandgap narrowing in heavily-doped epitaxial p-type silicon," *Microelectron. Eng.*, vol. 19, no. 1–4, pp. 691–694, Sep. 1992.

[25]   J. Wagner and J. A. del Alamo, "Band-gap narrowing in heavily doped silicon: A comparison of optical and electrical data," *J. Appl. Phys.*, vol. 63, no. 2, p. 425, 1988.

[26]   W. P. Dumke, "Band-gap narrowing from luminescence in p-type Si," *J. Appl. Phys.*, vol. 54, no. 6, p. 3200, 1983.

[27]   K. R. McIntosh and P. P. Altermatt, "A freeware 1D emitter model for silicon solar cells," in *2010 35th IEEE Photovoltaic Specialists Conference*, 2010, pp. 002188–002193.

[28]   A. Cuevas, P. A. Basore, G. Giroult-Matlakowski, and C. Dubois, "Surface recombination velocity of highly doped n-type silicon," *J. Appl. Phys.*, vol. 80, no. 6, p. 3370, 1996.

[29]   B. Min, H. Wagner, A. Dastgheib-Shirazi, A. Kimmerle, H. Kurz, and P. P. Altermatt, "Heavily doped Si:P emitters of crystalline Si solar cells: recombination due to phosphorus precipitation," *Phys. status solidi – Rapid Res. Lett.*, vol. 8, no. 8, pp. 680–684, 2014.

[30]   A. Dastgheib-Shirazi, M. Steyer, G. Micard, H. Wagner, P. P. Altermatt, and G. Hahn, "Relationships between Diffusion Parameters and Phosphorus Precipitation during the POCl3 Diffusion Process," *Energy Procedia*, vol. 38, pp. 254–262, 2013.

[31]   F. Schindler, M. C. Schubert, A. Kimmerle, J. Broisch, S. Rein, W. Kwapil, and W. Warta, "Modeling majority carrier mobility in compensated crystalline silicon for solar cells," *Sol. Energy Mater. Sol. Cells*, vol. 106, pp. 31–36, Nov. 2012.

[32]   M. A. Green, "Self-consistent optical parameters of intrinsic silicon at 300 K including temperature coefficients," *Sol. Energy Mater. Sol. Cells*, vol. 92, no. 11, pp. 1305–1310, Nov. 2008.

[33]   M. Rudiger, J. Greulich, A. Richter, and M. Hermle, "Parameterization of Free Carrier Absorption in Highly Doped Silicon for Solar Cells," *Electron Devices, IEEE Transactions on*, vol. 60, no. 7. pp. 2156–2163, 2013.

[34]   "The National Institute of Standards and Technology, Reference on Constants, Units and Uncertainty." [Online]. Available: http://physics.nist.gov/cuu/Constants/index.html.